Colloid Polym Sci 274:809–818 (1996)

ORIGINAL CONTRIBUTION

F. Aliotta
M.E. Fontanella
M. Sacchi
C. Vasi
G. La Manna
V. Turco-Liveri

About entangled networks of worm-like micelles: a rejected hypothesis

Received: 11 December 1995
Accepted: 29 January 1996

Dr. F. Aliotta (✉) · M.E. Fontanella
M. Sacchi · C. Vasi
Istituto di Tecniche Spettrscopiche del CNR
Salita Sperone 31
98166 Messina, Italy

G.L. Manna · V. Turco-Liveri
Dipartimento di Chimica-Fisica
Universita Palermo
Via Archirafi 26
90123 Palermo, Italy

Abstract We report new results from small-angle neutron scattering on d_{12}-cyclohexane/lecithin/water micellar solutions performed as a function of the water content (w_0), temperature (T) and dispersed phase volume fraction (ϕ). The data from dilute samples are interpretable in terms of the existence of giant cylindrical reverse micelles and are well fit with a core-shell model (that provides the micelle structure and dimensions) with values of 28 and 45 Å for the inner core and the outer shell radii, almost independent on temperature and concentration. Such a result could appear consistent with the current idea that worm-like micelles are living polymers. On the contrary, the appearance of a sharp interference maximum at high concentrations ($\phi > 0.15$) suggests arguments against the current hypothesis of an entangled network of giant flexible cylinders. Further arguments against the current hypothesis are given by the close similarity between the above described results and those from free of water micelles (for sure not cylinders). All the data are well fitted in terms of a unique model taking into account the micellar form factor plus a hard sphere structure factor. The data analysis suggests a micellar size distribution determined by the competition between concentration and interaction effects on which temperature plays not a minor role. Following our results, the current hypothesis of a gel structure in terms of an entangled network can be assumed as wrong and some caution has to be taken in assuming worm-like micelles as living polymers.

Key words Living polymers – gels – reverse micelles – SANS

Historical background

About ten years ago, a new class of organogels from water-in-oil microemulsions was for the first time detected [1]. In their pioneering work, R. Scartazzini and P.L. Luisi reported the discovery of a sol–gel transition in a soybean lecithin/organic solvent/water microemulsion. With surprise they found that gels could be obtained at relativity low concentration of the surfactant without addition of gelatin or other macromolecular compounds. The elucidation of the observed phenomenon represents a challenging enterprise because the gel structure could not be explained in terms of the existence of a chemically cross-linked polymeric network. The new result triggered a number of rheological investigations in order to obtain useful information about the mechanism driving the observed sol–gel transition [2, 3]. There were detected at least 50 different solvents in which the viscoelastic behavior is observed. At the same time, it was found that several

Colloid & Polymer Science, Vol. 274, No. 9 (1996)

solvents are not able to form lecithin gels. This should mean that the physical properties of our systems are solvent dependent. It soon became clear the main role played by water on the gel structure: the viscosity of a solution of lecithin in a good solvent undergoes an abrupt increase upon addition of small quantities of water. Further addition of water will increase the value of the viscosity by several orders of magnitude, until a maximum water content is reached; after that the viscosity will fall. The maximum allowed water content turned out to be solvent dependent. An additional experimental remark concerning the degree of purity of the soybean lecithin: soybean of insufficient purity does not yield gels.

In summary, when a good solvent is detected, the establishment of the gel structure seems to be determined by the dispersed phase volume fraction, ϕ, the water content, w_0 (w_0 = number of water molecules per surfactant molecule) and the temperature, T. Besides the three parameters ϕ, w_0 and T, other not well known experimental conditions could play a role: i.e., some discrepancies between the viscosity values obtained in different experiments could be tentatively imputed to a different concentration of impurities in the starting lecithin.

There are a number of possible reasons for the observed high viscosity. One could be the formation of liquid crystalline mesophase, but observation of polarising microscopy detected no birefringence, neither ^{31}P-NMR nor ^{2}H-NMR measurements [4, 5] showed any signs of anisotropy. Another possibility was the existence of a cubic liquid crystalline phase but small-angle neutron scattering (SANS) and small-angle x-ray scattering did not support the existence of such a local order. It became certain that our system is a completely isotropic solution. So the conclusion was reached that there had to be a macromolecular structure which is responsible for the high viscosity and, as a consequence, many efforts were devoted to the search for this particular structure.

At that time, Cates had developed a theoretical study of the dynamics of stress relaxation in a dense system of living polymers [6]. In that work, linear chain polymers were taken into consideration, able to break and recombine on experimental time scales. In the model, simple reaction kinetics were assumed in which a chain can break with uniform probability per unit time and unit length at all points in the chemical sequence and two chains can combine with a rate proportional to the product of the concentrations. The model furnished a chain length distribution exponential with mean $\bar{L}$. In such a way, $\bar{L}$ turned out to be concentration dependent but it was implicitly assumed that it is not influenced by excluded volume effects. Two relevant time scales were detected for the stress relaxation mechanism, namely τ_{rep}, the reptation time of a polymer of length $\bar{L}$, and τ_{break}, the mean time for such a chain to break in two pieces. Of course, when $\tau_{break} \gg \tau_{rep}$, the Cates model collapses into the de Gennes reptation theory for molten polymers [7].

On this basis a simple model for the structure of reverse micelles as a function of the water content was proposed: addition of water induces the one-dimensional growth of the small lecithin aggregates into rod like aggregates; upon further addition of water, rods grow into long and flexible reverse micelles. After a critical lecithin volume fraction, ϕ^*, the micelles start to overlap and entangle in a transient network very similar to the local arrangement hypothesised by Cates for living polymers.

The close analogy between worm-like micelles and living polymers was stressed by R. Messager and coworkers [8] that reported the first self-diffusion measurements in the semidilute regime performed with fringe-pattern photobleaching-techniques.

From that time, such working hypothesis was taken as good and all the experimental results were analyzed successfully within this framework. SANS experiment and elastic light scattering results [9] were analyzed under the assumption of the existence of cylindrical micelles and under the assumption of an exponential size distribution in agreement with the indication of the Cates model.

The data analysis in terms of locally cylindrical structures was able to furnish consistent evaluation for the mean length and the flexibility of the worm like micelles.

Also, our group was extensively involved in studying the statical and dynamical properties of such kind of system. Brillouin scattering [10], depolarized Rayleigh scattering [11, 12], ultrasonic [11, 12] and dielectric [12, 13] measurements were successfully interpreted in terms of the existence of a distribution of relaxation times, in agreement with the hypothesized hierarchy of structures. The volume fraction dependence of the hyperacoustic parameters and the results from a quasi elastic incoherent neutron scattering experiment [14] were interpreted consistently with an exponential micelle size distribution with a mean value scaling with $\phi^{1/2}$.

Schurtenberger and co-workers performed a number of further data analyses of SANS and elastic light scattering results in terms of the assumed polymer like behavior [15–17]. In particular, they successfully tried the application of results from conformation space renormalization group theory to worm-like micelles. They showed the possibility of obtaining information from static light-scattering experiments on the concentration dependence of both micellar size distribution and the intermicellar interaction effects. For low scattering angles, where $Q\xi_h \ll 1$ (being ξ_h the static correlation length), their data appear to follow a simple Lorentzian law, in agreement with the assumed similarity with a neutral polymer-like system. Such an occurrence allowed them to determine ξ_h and, for

data at low concentrations ($\phi < \phi^*$), the gyration radius. In any case, the behavior of the scattered intensity at high Q values diverges from the simple Lorentzian law, indicating that the model could lead to errors when applied to samples with very pronounced micellar growth. The data in the semidilute regimes were fitted consistently with scattering pattern from polydisperse semiflexible chains with excluded volume effects and an exponential size distribution.

Very recently [18], we performed a SANS experiment on d_{12}-cyclohexane/lecithin/water micellar solution as a function of ϕ, at fixed water content ($w_0 = 9.7$), crossing ϕ^* ($\phi^* \cong 0.015$). The data for $\phi < \phi^*$ are well fit with a concentric cylinders model (core-shell) with values for the mean micellar contour length and for the cross-sectional radii in good agreement with previous findings.

Surprisingly, the data from samples at $\phi > \phi^*$ showed a strong interference maximum not interpretable, in a consistent way, with the assumption of an entangled network of giant worm-like micelles whose mean length scales with ϕ follow the indication of the Cates model. Such an occurrence strongly suggested caution in applying analogies between worm-like micelles and polymer solutions, when excluded volume effects become relevant.

In this paper, we present new results from a SANS experiment on the same system as a function of ϕ, w_0 and T performed in order to test the influence of these three parameters on the mean micelle size and on the micellar size distribution. We will show that the mean size of the micelles is determined by the competition between the equilibrium kinetics of the micelle breaking and reforming mechanisms, driving the growth of the micellar length with ϕ, and intermicellar interactions, which put strong limitations on the growth process itself. Furthermore, we will show how, at high volume fraction of the dispersed phase, excluded volume fraction effects can induce the existence of a preferred micellar size. This means that the micellar size distribution could be exponential only when excluded volume interactions are negligible and that the hypothesis of an entangled network of worm-like micelles as a possible structure for the gel has to be rejected.

Materials and methods

High purity (97%) soybean lecithin was purchased by Lucas Meyer (Epikuron 200) without further purification procedures. The lecithin was dissolved, under continuous stirring at 20 °C, in cyclohexane-d_{12} (99.5% isotopic purity from Aldrich) to obtain a lecithin volume fraction $\phi = 0.3$. Then water was added to obtain samples at different water content ($w_0 = 0$, 4.93, 10, 12.2). Samples with different concentrations were obtained by dilution ($0.002 \leq \phi \leq 0.2$).

SANS measurements were made using the LOQ small-angle instrument at the ISIS facility (Rutherford Appleton Laboratory). The covered scattering Q vector range was 8.5×10^{-3} Å$^{-1} \leq Q \leq 2.1 \times 10^{-1}$ Å^{-1}. Samples were placed in rectangular quartz cells with a path length of 1 mm. Measurements were performed at the temperatures of 14 °, 20.2°, 30° and 38 °C. Scattered neutrons were collected on a 64×64 array detector. Each two-dimensional set of row scattering data was corrected for detector background, for empty cell scattering, solvent scattering, sample thickness, transmission and radially averaged by using standard procedures. The intensity data were converted to an absolute differential scattering cross-section per unit solid angle, per unit volume of material $I(Q)$ (cm^{-1}) using a standard isotropic scatterer of known scattering cross-section.

Results and discussions

In Fig. 1 the normalized scattering data at different volume fractions are reported for the $w_0 = 0$ samples at the different temperatures investigated. It is easy to observe that two main effects are driving the appearance of a structure factor contribution: i) the increasing of the temperature; ii) the increasing of the lecithin volume fraction ϕ.

The data we are dealing with at the moment, concern a simple two-component system and, following the model proposed by Schurtenberger and co-workers [2], we should be in the presence of a disperse system of globular lecithin reverse micelles: it will be the addition of the third component, water, that will trigger a sphere-to-rod transition and then the formation of giant cylindrical reverse micelles.

Because the main effect of increasing the temperature should be the lowering of the mean micellar size (determined by the equilibrium kinetics between the breaking and reforming mechanisms of the micelles), one could deduce that, from this point of view, both an increase of T or ϕ should lead to the same result. As a consequence, the appearance of the observed structure factor should be connected with an increasing of the micelle population not only determined by the increasing of ϕ but also by the lowering of the mean micellar radius. At the same time, one can expect that the two effects are not independent: an increasing of the surfactant volume fraction should induce a change on the breaking and reforming equilibrium kinetics.

Such an argument is strongly supported by the T-dependence of the $I(Q)$ vs Q curves at the high concentration investigated. In such a case, as can be observed in Fig. 1, the shape of the spectra appears almost independent from temperature, the main effect being a shift of the

Colloid & Polymer Science, Vol. 274, No. 9 (1996)

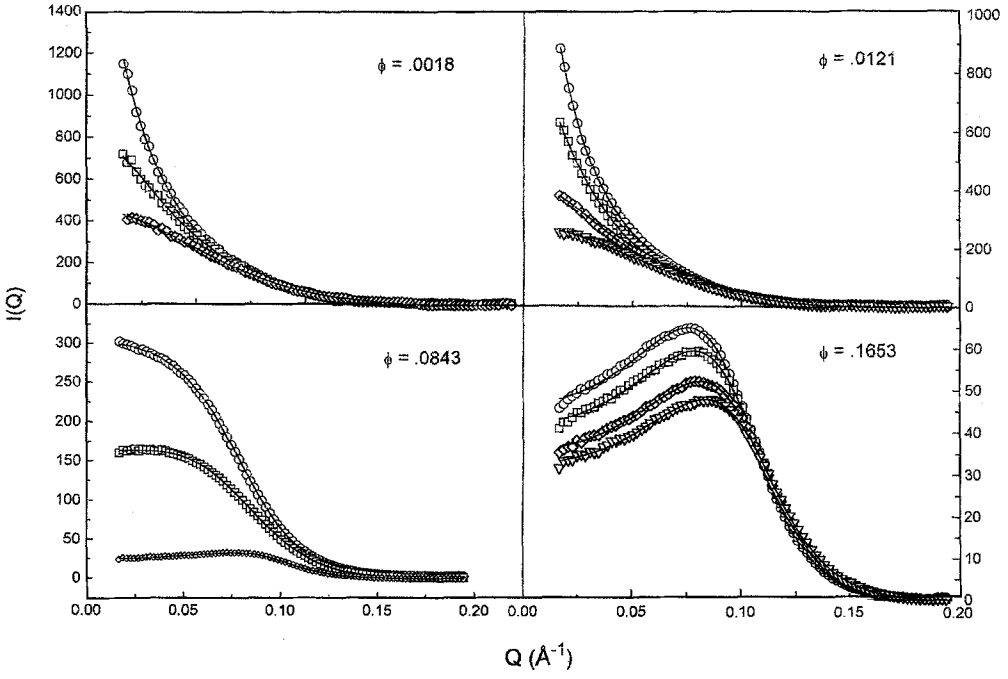

Fig. 1 Normalized scattering intensity for samples at $w_0 = 0$. Symbols: ○ 14 °C, □ 20.2 °C, ◇ 30 °C, ▽ 38 °C. Continuous lines interacting polydisperse hard spheres model

interference peak towards higher Q-values when T is increased. Such an occurrence seems to be in agreement with the hypothesis of a preferred micellar size at high concentration, essentially determined by excluded volume effects and on which temperature plays a minor role.

If one assumes a spherical form factor for the micellar aggregates and a hard sphere interaction for the structure factor contribution, the data should be fit when the appropriate expression for the size distribution function is found. In agreement with what was assumed above the experimental data can be reproduced by a law [19]

$$I(Q) \propto P(Q) \frac{1}{1 + \frac{8v_0}{v_1} \cdot \varepsilon \Phi(DQ)}, \tag{1}$$

where ε is a constant that, in practice, can be taken as equal to 1, v_0 is the volume of the interacting particle, v_1 is the average volume assigned to each particle, $\Phi(QD)$ is the potential energy function and D is the average micellar distance. $P(Q)$ is the scattering form factor for polydisperse spherical particles with size distribution function $n(R)$

$$P(Q) \propto \int_0^\infty \int_0^\infty \sqrt{n(R_1)n(R_2)}\Phi(QR_1)\Phi(QR_2) \times \delta(R_1 - R_2)dR_1dR_2 . \tag{2}$$

The $\Phi(x)$ functions in (1) and (2) are given by

$$\Phi(QR) = 3\frac{\sin(QR) - QR\cos(QR)}{Q^3R^3},$$

and $n(R_1), n(R_2)$ represent the density numbers for particles of radius R_1 and R_2 respectively.

The first problem concerns the choice of a suitable form for the $n(R)$ function. First of all, we tried an exponential distribution function $n(R) = \exp[-R/\bar{R}]$. Such a choice turned out to be almost adequate for samples at low ϕ values but failed to fit with samples at $\phi > \phi^*$, in agreement with the above hypothesis that excluded volume effects have to change the size distribution function.

Furthermore, also for dilute samples, Eq. (2) fails to fit with the experimental data at the higher Q-values. In effect, the problem could stem from the lower integration limit ($R = 0$) that implies the existence of particles smaller than those allowed by physical considerations. As a consequence, we need to find a cut-off value, at low R-values, for the $n(R)$ function. In order to obtain information about the size of the minimum allowed radius for lecithin micelles, we preliminary fit the high Q-portion of all the spectra with a simple monodisperse sphere model. A mean value for the minimum radius of the micelles was found of about 20 Å. After that, following the above considerations, we tentatively adopted a Weibull density function as size

Table 1 Results of the fitting procedure with polydisperse interacting hard sphere model for samples at $w_0 = 0$. $\bar{R}$, mean micellar radius; D, mean intermicellar distance; b, see Eq. (3); $8v_0/v_1$, see Eq. (2)

T (°C)	ϕ	$\bar{R}$(Å)	D(Å)	b	$8v_0/v_1$
14.0	0.002	83.45	–	1.00	–
20.2	0.002	26.28	–	1.02	–
30.0	0.002	10.02	–	1.01	–
14.0	0.012	109.71	–	1.00	–
20.2	0.012	54.39	–	1.00	–
30.0	0.012	29.21	–	1.33	–
38.0	0.012	17.01	–	1.60	–
14.0	0.084	35.75	61.42	5.62	1.09
30.0	0.084	29.71	56.04	6.88	3.02
14.0	0.165	24.81	55.88	5.57	2.46
20.2	0.165	24.64	54.53	5.75	2.60
30.0	0.165	21.25	53.19	4.63	2.68
38.0	0.165	20.91	52.06	4.87	2.73

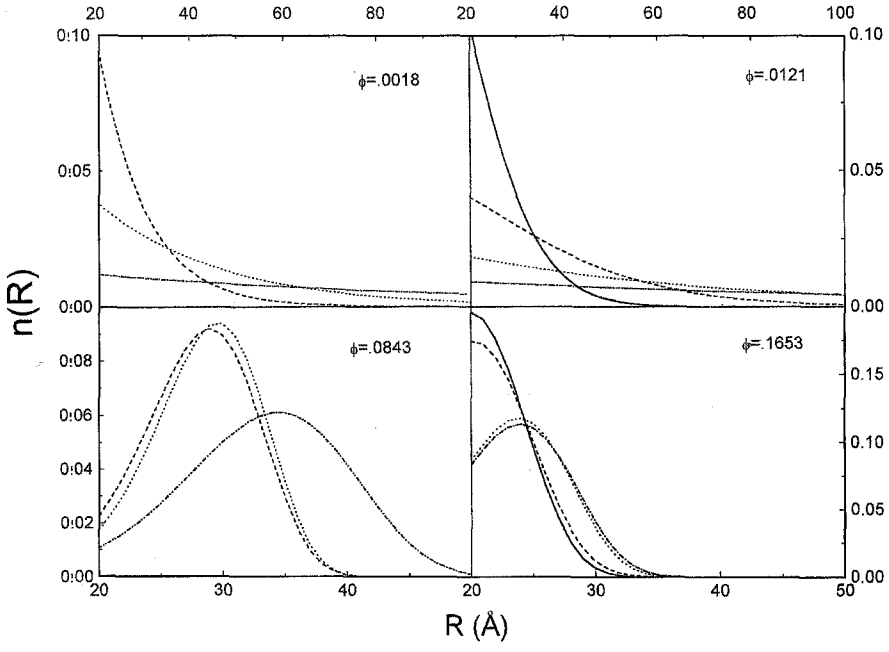

Fig. 2 Micellar size distribution function for samples at $w_0 = 0$ (see text for details). Dashed – dotted lines $T = 14\,°C$, dotted lines $T = 20.2\,°C$, dashed lines $T = 30\,°C$, continuous lines $T = 38\,°C$

distribution function

$$n(R) = A(R/\bar{R})^{b-1}\exp[-(R/\bar{R})^b] \,. \quad (3)$$

Equation (3) could be adequate for our purposes since it collapses to a simple exponential behavior when the parameter b takes the value of 1 while, for increasing b value, changes in a localized distribution around the mean value $\bar{R}$. In such a way, an increasing of the parameter b to values significantly higher than 1 will mark the transition from a regime in which the growing up of the micellar radius is simply driven by equilibrium kinetics to a new one, in which the process is hindered by excluded volume effects (see Table 1).

When Eq. (3) and the low R value cut-off are inserted in Eq. (2) all the experimental spectra can be fit with very high accuracy (see continuous lines in Fig. 1). The fitting procedure furnishes the values for the parameters R, D, b and the excluded volume factor $8v_0/v_1$. The fitting results are reported in Table 1.

In Fig. 2 are reported the resulting size distribution functions for the different concentrations at each temperature investigated. It is easy to observe that an increase of the temperature induces a narrowing of the $n(R)$ function. The same effect appear to be induced by an increase of the concentration but, in this case, also a preferred micellar size is originated, in agreement to that discussed above. To

Colloid & Polymer Science, Vol. 274, No. 9 (1996)

find a theoretical background able to explain our results, we can refer to the work of Blankschtein and co-workers [20].

Following the formalism of ref. [20], we can take into consideration a solution of N_L lecithin molecules and N_S solvent molecules in thermodynamic equilibrium at temperature T and pressure p. The self-association of lecithin molecules produces a distribution $n(R(N))$ of micellar sizes, where $R(N)$ is the mean radius of micelles with aggregation number N. The Gibbs free energy, G, of the solution can be modeled as consisting of three additive parts G_f, G_m and G_{int} representing the micelle formation, micellar aggregate mixing, and inter-aggregate interaction contributions, respectively.

The three contributions can be written in the form

$$G_f = N_s\mu_s^0 + \sum_N n(R(N))\bar{\mu}_N^0 ,$$

where $\mu_s^0(T, p)$ is the free energy change of the solution induced by the addition of a solvent molecule to the pure solvent and $\bar{\mu}_N^0(T, p)$ represents the change in the free energy of the solution when a single aggregate of size $R(N)$ is placed at a given position in the pure solvent;

$$G_m = k_B T\left[N_s\ln(X_s) + \sum_N n(R(N))\ln(X_N)\right],$$

where $X_S = N_S/(N_S + N_L)$, $X_N = n(R(N))/(N_S + N_L)$ and k_B is the Boltzmann constant

$$G_{int} = -(1/2)\sum_N n(R(N))U_N ,$$

where $U_N = U\sum_J f_{NJ}\rho_J$.

In this last expression each N-mer is described as interacting with an average local potential U_N produced by the other J-mers. Such a potential is proportional to the J-mer concentration ρ_J. The coupling constant f_{NJ} describes how the average interaction between N-mer and a J-mer depends on the number of lecithin molecules in each of them.

In such an approach, micellar aggregates of different sizes were treated as independent chemical species, but actually the aggregates are continually exchanging lecithin molecules with one another. Such exchanges can be described as a multiple chemical equilibrium between the members of the micellar size distribution. At the thermodynamic equilibrium the chemical potential per lecithin molecule has to be independent from the aggregate, namely $\mu_N/N = \mu_1$ for each N. When the chemical potentials for pure solvent and for each N-mer are calculated it is possible to obtain the mole fraction X_N of the various species of the micellar size distribution.

$$X_N = (X_1)^N\exp[-\beta(\mu_N^0 - N\mu_1^0)]\exp\left\{\left[\frac{\beta C\gamma}{1 + (\gamma - 1)X}\right]\times\left[\sum_J (f_{NJ} - Nf_{1J})X_J\right]\right\}, \quad (4)$$

where $\beta = 1/K_B T$, $C(T, p) = [U(T, p)/\Omega_L]$ and $\gamma = \Omega_L/\Omega_s$ being Ω_L and Ω_s the effective volumes of a lecithin and an organic solvent molecule respectively.

Of course the total number of lecithin molecules in solution is given by $N_L = \sum_N Nn(R(N))$, or, referring to the mole fraction, $X = \sum_N X_N n(R(N))$.

From Eq. (4) it is clear that the micellar size distribution is strongly influenced by three physical factors: i) $(X_1)^N$, taking into account the large entropic disadvantage of translating N lecithin molecules as a single cluster, ii) the first Boltzmann factor, representing the enhancement of the micellar configuration induced by assembling N lecithin molecules into a single N-mer; iii) the last Boltzmann factor, describing how the micellar size distribution can be affected by intermicellar interactions. The crucial point concerns the adoption of a suitable form for the coupling constants f_{NJ}. In ref. [20], the authors showed that the choice $f_{NJ} = NJ$, implying that $f_{NJ} = Nf_{1J}$ reduces the second Boltzmann factor to unity. Such a result implies that intermicellar interactions do not affect the micellar size distribution.

Of course, this is not our case, as clearly shown by the micellar size distribution reported in Fig. 2, or by Fig. 3,

Fig. 3 First moments of the size distribution functions reported in Fig. 2. Continuous lines are only guides for the eye

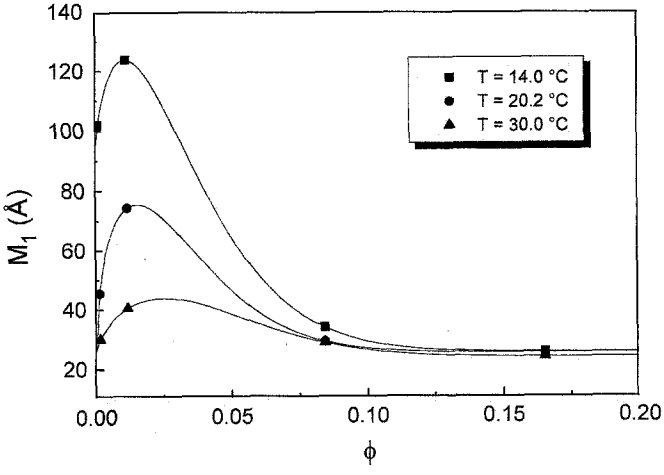

where the first moments of the size distribution functions are reported.

$$M_1 = \frac{\int_{R_{min}}^{R_{max}} Rn(R)\,dR}{\int_{R_{min}}^{R_{max}} n(R)\,dR},$$

R_{min} and R_{max} being the minimum and the maximum allowed radii for the micelles respectively.

The same behavior is obtained for the second moment of the distributions. It is easy to observe that, at low values, ϕ acts essentially as $1/T$: an increasing of ϕ or $1/T$ will induce both a growth in the micellar size and an increase of the micellar size distribution width. Such an occurrence should correspond to a situation in which polidispersity is essentially determined by the breaking and reforming mechanisms for the micelles [16].

But the situation appears quite different at higher ϕ values: intermicellar interaction effects become dominant, a serious cut-off is imposed to the maximum allowed micellar radius and, as a consequence, the width of the distribution narrows. At high ϕ values the mean micellar radius and polydispersity are essentially driven by excluded volume effects.

To obtain a theoretical expression for the detected size distribution functions, we should to determine the sequence of chemical potential $\{\mu_N^0\}$ as a function of N and the dependence of the coupling constants $\{f_{NS}\}$ on N and S. Such a goal could be obtained by a detailed knowledge of the ϕ and T dependence of the various moments of the size distribution function. Further measurements are actually in planning with this aim.

When water is added to our samples, a unidimensional growth of the micelles should be detected, in agreement with the current theories.

In a recent paper [18], we reported about the existence of an interference maximum at high ϕ concentrations that cannot be explained on the basis of random cross-linked polymer like network models. Such a result suggested the existence of strong limitations imposed by intermicellar-interactions on the growth process of the aggregates. As a consequence, we tried to fit the $I(Q)$ vs Q curves for lecithin/cyclohexane/water systems with Eq. (2) where a core-shell model was adopted for the form factor of the cylindrical particles

$$P(Q) \propto \int_0^{\pi/2} \sin\beta |(\rho_1 - \rho_2) V_a G(Q, \beta, a) + (\rho_2 - \rho_0) V_b G(Q, \beta, b)|^2 d\beta\,, \quad (5)$$

where ρ_1, ρ_2 and ρ_0 are the neutron scattering length densities of the inner cylinder, outer coating and solvent respectively, a and b are the core radius and the outer radius of the micelles, $V_a = \pi a^2 L$ and $V_b = \pi b^2 L$ represent the core and the micelle volume respectively, the function

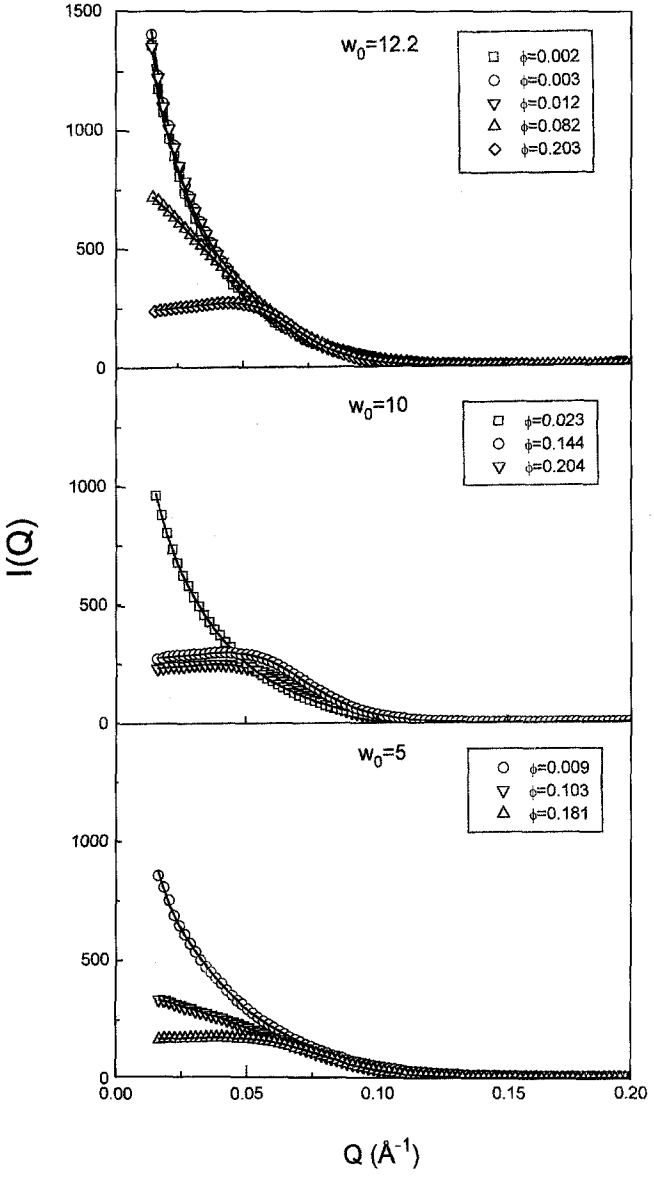

Fig. 4 Normalized scattering intensity for samples at $T = 20.2\,°C$. Continuous lines: concentric cylinders model with excluded model contribution

$G(Q, \beta, x)$ is defined as

$$G(Q, \beta, x) = \frac{\sin(QH\cos\beta) 2J_1(Qx\sin\beta)}{(QH\cos\beta)(Qx\sin\beta)},$$

where $H = L/2$, J_1 is the first order Bessel function and β is the angle between the Q-vector and the axis of the micelles.

Of course, the adoption of Eq. (5) as the cylinder form factor fails to take into account the micellar polydispersity. In any case, as was discussed in detail in ref. [18], the

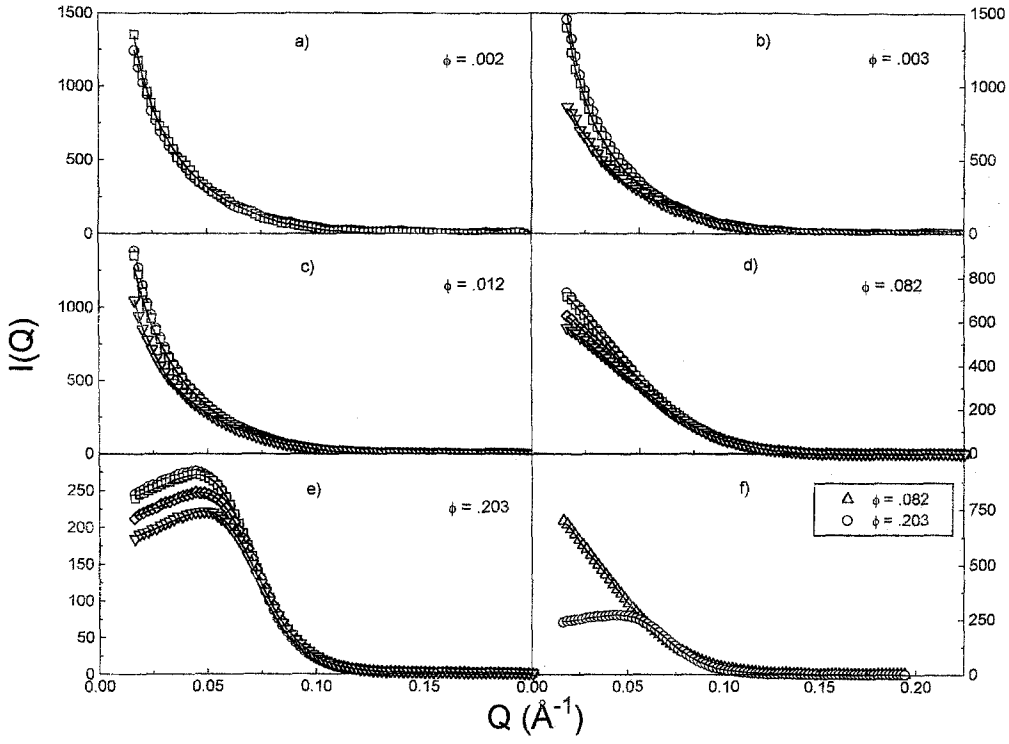

Fig. 5 Normalized scattered intensity for samples at $w_0 = 12.2$. Symbols: a)–e) ○ 14 °C, □ 20.2 °C, ◇ 30 °C, ▽ 38 °C, f see inset. Continuous lines: a)–e) concentric cylinders model with excluded model contribution, f) interacting polydisperse hard spheres model

limited exchanged Q-range explored in our experiments does not allow a clear determination of the size distribution function. Equation (5) appears able to fit with our experimental results in excellent agreement with the limitation that the obtained length values have to be taken just as an indication of the average contour length.

In Fig. 4 are reported the experimental data at $T = 20$ °C for different ϕ values, as a function of the water content w_0.

The effect of the temperature is well shown in Figs. 5a)–e) where the results from samples at $w_0 = 12$ are reported, as a function of T, for different volume fractions of the dispersed phase. In Table 2, we report the obtained values of the parameters involved in the fitting procedure with Eq. (5). The reported values are obtained under assumption of scattering length density values $\rho_1 = -0.56$, $\rho_2 = 7.1$, $\rho_0 = 6.7$ ($\times 10^{10}$ cm^{-2}) independently by concentration and temperature (see ref. [18] for details). It can be easily observed that the ϕ and T dependence of $I(Q)$ vs Q curves reported in Figs. 4 and 5 give evidence for a structural evolution very close to the one detected for samples at $w_0 = 0$.

The similarity between the two sets of data becomes quite evident at the higher ϕ values. In such a case, in fact, the same interference peak is observed, suggesting the existence of a preferred inter-particles correlation distance. The same local structural arrangement is imposed with no regard to the water content. The only effect induced by addition of water is a shift of the peak position toward lower Q-values, consistent with an increase of the mean micellar gyration radius, due to higher volumes of the water pools. The obtained values for the cross-sectional radii of the inner core and the outer shell, reported in Table 2 seem to be almost temperature and concentration independent, in good agreement with previous results [18].

Furthermore, a monotonic increase of the micelle contour length is obtained, at $\phi < \phi^*$, that could be in good agreement with previous findings in the literature. If one could extrapolate the observed behavior at $\phi > \phi^*$, our results should be consistent with the formation of an entangled network of giant worm-like micelles that should induce a low Q-Lorentzian behavior for the scattering profile (see, e.g., ref [17]).

On the contrary, the appearance of an interference peak has led us to refuse such a working hypothesis, respective evidence for a micellar growth process strongly hindered by intermicellar interactions. The results of the fitting procedure with Eq. (5), at $\phi > \phi^*$, clearly give evidence for the dramatic shortening of the average length of the cylindrical micelles when the interactions are no longer negligible.

Table 2 Results of the fitting procedure with core-shell cylindrical model and hard-sphere interaction for d_{12}-cyclohexane/lecithin/water systems at different concentrations and temperatures. *a*, inner core radius; *b*, outer shell radius; *L*, average micellar length; connected structure correlation distance; $8v_0/v_1$, see Eq. (2)

ϕ	b(Å)	a(Å)	L(Å)	D(Å)	$8v_0/v_1$
$w_0 = 12.2$, $T = 14.0\,^\circ$C					
0.002	39.0 ± 0.3	26.6 ± 0.2	728 ± 17	–	–
0.003	38.2 ± 0.3	27.7 ± 0.2	1471 ± 37	–	–
0.012	41.8 ± 0.3	27.7 ± 0.2	1980 ± 50	–	–
0.082	39.6 ± 0.3	28.2 ± 0.2	165 ± 4	103.8	0.73
0.203	38.1 ± 0.3	28.6 ± 0.2	75 ± 2	81.6	1.81
$w_0 = 12.2$, $T = 20.2\,^\circ$C					
0.002	36.9 ± 0.3	27.1 ± 0.2	1440 ± 36	–	–
0.003	38.4 ± 0.3	27.0 ± 0.2	1335 ± 33	–	–
0.012	40.0 ± 0.3	27.6 ± 0.2	1570 ± 39	157.0	0.21
0.082	40.4 ± 0.3	28.5 ± 0.2	163 ± 4	103.7	0.70
0.203	38.8 ± 0.3	28.3 ± 0.2	81 ± 2	81.0	1.99
$w_0 = 12.2$, $T = 30.0\,^\circ$C					
0.082	42.9 ± 0.3	28.4 ± 0.2	162 ± 4	103.8	0.73
0.203	34.9 ± 0.3	28.6 ± 0.2	74 ± 2	80.0	1.85
$w_0 = 12.2$, $T = 38.0\,^\circ$C					
0.003	40.7 ± 0.3	26.2 ± 0.2	161 ± 4	661.3	1.00
0.012	44.4 ± 0.3	28.5 ± 0.2	444 ± 11	553.2	0.24
0.082	64.5 ± 0.3	26.6 ± 0.2	165 ± 4	107.4	0.63
0.203	43.3 ± 0.3	28.4 ± 0.2	73 ± 2	79.5	1.90
$w_0 = 5$, $T = 20.2\,^\circ$C					
0.009	54.0 ± 0.3	25.6 ± 0.2	1553 ± 28	–	–
0.103	40.5 ± 0.3	25.4 ± 0.2	137 ± 3	87.9	0.91
0.181	49.2 ± 0.3	26.4 ± 0.2	77 ± 2	69.6	1.36
$w_0 = 10$, $T = 20.2\,^\circ$C					
0.023	42.6 ± 0.3	27.6 ± 0.2	1920 ± 46	–	–
0.144	44.7 ± 0.3	28.2 ± 0.2	74 ± 2	77.6	1.45
0.204	44.1 ± 0.3	28.6 ± 0.2	75 ± 2	80.7	1.34

At the higher ϕ value the cylinder length is so short as to be comparable with the cross-sectional diameter (see Table 2). This means that, at least under such extreme condition, it would be difficult to talk about cylinders. The hypothesis of spherical aggregates very similar to those revealed for lecithin cyclohexane solution should appear more adequate.

Table 3 Results of the fitting procedure with polydisperse interacting hard sphere model for samples at $w_0 = 12.2$, $T = 20\,^\circ$C. $\bar{R}$, mean micellar radius; *D*, mean intermicellar distance; *b*, see Eq. (3); $8v_0/v_1$, see Eq. (2)

ϕ	$\bar{R}$(Å)	D(Å)	b	$8v_0/v_1$
0.002	162.14	–	1.00	–
0.003	138.91	–	1.00	–
0.012	102.72	–	1.19	–
0.082	41.62	304.8	4.76	0.32
0.203	41.84	81.0	6.49	1.95

We tried to fit our experimental results, at $\phi > \phi^*$, with the polydisperse interacting hard sphere model. In Fig. 5f) are reported, as continuous line, the results of such a fitting for the samples at $w_0 = 12.2$ and $T = 20.2\,^\circ$C. The corresponding parameters are reported in Table 3. From Fig. 5f) it turns out quite evident that the polydisperse interacting hard sphere model appears able to fit with our experimental data in very good agreement.

In summary, we can conclude that, at a concentration $\phi > \phi^*$, there is no meaning in talking about worm-like micelles.

Of course the proposed local arrangement of spherical particles (see Fig. 6a)) could be accepted for the $w_0 = 0$ samples, but cannot be simply translated to the case of samples with a large content of water. A possible picture of the situation detected in this last case could be represented by a bicontinuous structure (see Fig. 6b)) with obvious reinterpretation of the obtained fitting parameters.

The bicontinuous structure, induced by the presence of water, could be able to explain the observed sol–gel

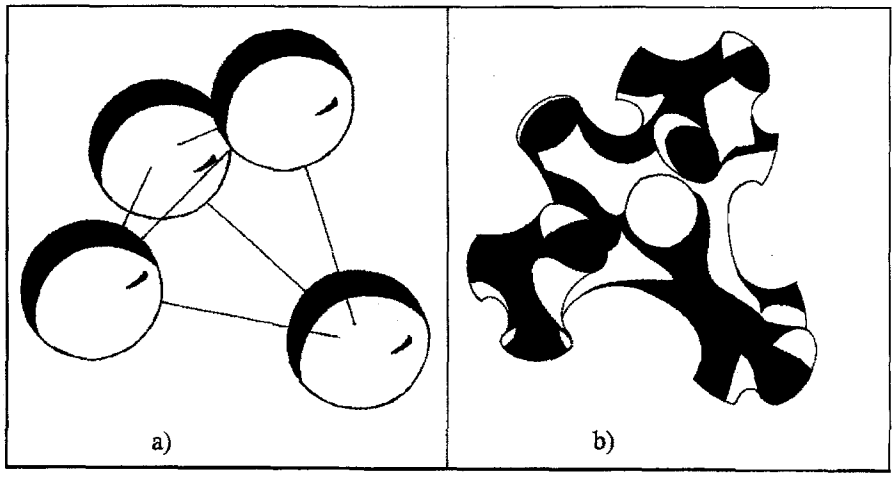

Fig. 6 Local arrangements consistent with the fitting results for $\phi = 0.27$ sample. a) Closed packed arrangement of spherical micelles. b) Bicontinuous structure. Note that both pictures show the same tetrahedral symmetry (see text)

transition. In any case, the true structure of the gel is still an open question.

At the moment, we can only conclude that the existence of worm-like micelles able to grow monotonically over distances greater than the entanglement length is not confirmed and that the hypothesis of polymer-like entangled network should be definitely refused.

Conclusions

Our results, putting into evidence the close similarity between the scattering profiles from lecithin in oil-microemulsion and lecithin/water/organic solvent reverse micelles, at least at high volume fractions, unambiguously show that the gel structure cannot be explained in terms of the existence of an entangled network of giant worm-like micelles. It was also shown that even in the diluted regime, some caution should be taken in hypothesizing analogies between our system and living polymers.

The elucidation of the microscopic mechanism driving the observed sol–gel transition remains an open question. Further experimental works need to find an adequate thermodynamic approach to the formulation of a working theoretical model.

References

1. Scartazzini R, Luisi PL (1988) J Phys Chem 92:829
2. Schurtenberger P, Scartazzini R, Luisi PL (1989) Rheol Acta 28:372
3. Luisi PL, Scartazzini R, Haering G, Schurtenberger P (1990) Colloid Polymer Science 268:356
4. Lindman B, Stilbs P (1985) Physics of Amphiphiles: Micelles, Vesicles and Microemulsions. Degiorgio V, Corti M (eds) North-Holland Physics Publishing, pp 94
5. Svärd M, Schurtenberger P, Fontell K, Jönsson B, Lindman B (1988) J Phys Chem 92:2261
6. Cates ME (1978) Macromolecules 20: 2289
7. de Gennes PG (1972) J Chem Phys 55:572
8. Messanger R, Ott A, Chatenay D, Urbach W, Langevin D (1988) Phys Rev Lett 60:1410
9. Schurtenberger P, Magid LJ, King SM, Lindner P (1991) J Phys Chem 95:4173
10. Aliotta F, Fontanella ME, Squadrito G, Migliardo P, La Manna G, Turco-Liveri V (1993) J Phys Chem 97:6541
11. Aliotta F, Fontanella ME, Magazu' S, Vasi C, Crupi V, Maisano G, Majolino D (1992) Mol Cryst Liq Cryst 212:255
12. Aliotta F, Fontanella ME, Magazù S, Maisano G, Majolino D, Migliardo P (1992) Prog Colloid Polym Sci 89:253
13. Aliotta F, Fontanellla ME, Galli G, Lanza M, Migliardo P, Salvato G (1993) J Phys Chem 97:733
14. Aliotta F, Fontanella ME, Vasi C, Sacchi M, La Manna G, Turco-Liveri V (1994) Nuovo Cimento 16D:771
15. Schurtenberger P, Cavaco C (1993) J Phys II France 3:1279
16. Schurtenberger P, Cavaco C (1994) J Phys Chem 98:5481
17. Schurtenberger P, Cavaco C (1994) J Phys II France 4:305
18. Aliotta F, Fontanella ME, Sacchi M, Vasi C, La Manna G, Turco-Liveri V, to appear on J Mol Struct (1996)
19. Guiner A, Fournet G (1955) Small Angle x-Ray Scattering. J Wiley: New York
20. Blankschtein D, Thurston GM, Benedek GB (1986) J Chem Phys 85:7268